Amirkabir University of Technology
(Tehran Polytechnic)
Vol. 45, No. 1, spring 2013, pp. 51- 58

Amirkabir International Journal of Science& Research
(Electrical & Electronics Engineering)
(AIJ-EEE)

Power Amplifier Linearization Using Six-port Receiver for DVB-S2 Satellite Communications

R. Ebrahimi Ghiri[1], A. Mohammadi[2]*, A. Abdipour[3], R. Mirzavand[4]

1- M.Sc. Student, Department of Electrical Engineering, Amirkabir University of Technology, Tehran, Iran
2- Professor, Department of Electrical Engineering, Amirkabir University of technology, Tehran, Iran
3- Professor, Department of Electrical Engineering, Amirkabir University of technology, Tehran, Iran
4- Assistant Professor, Department of Electrical Engineering, Amirkabir University of technology, Tehran, Iran

ABSTRACT

A digital look-up table adaptive predistortion technique using a six-port receiver for power amplifier linearization is presented. The system is designed in Ka-band for a DVB-S2 satellite link. We use a six-port receiver at the linearization loop in place of classic heterodyne receivers. The six-port receiver is implemented by the use of passive microwave circuits and detector diodes. This approach highly reduces cost and complexity of the linearization system. The fabrication results of a five-port receiver operating in 23–29 GHz is presented in this paper. The simulation results confirm suitability of using this architecture in the power amplifier linearization loop. The third order intermodulation products and the fifth order intermodulation products reduce about 43 dB and 25 dB respectively, after linearization of the power amplifier. The resulting spectrum of the output signal shows significant reduction of the intra-system interference to the adjacent networks which is mainly due to the nonlinearity effects of the power amplifier.

KEYWORDS

Ka-band, Digital Predistortion, Linearization, Six-port, Five-port

* Corresponding Author, Email: abm125@aut.ac.ir

1- INTRODUCTION

The linearization of Power Amplifier (PA) is a critical issue in digital wireless communications. Nonlinearity in PA causes adjacent channel interference and intermodulation distortion. Several linearization techniques for PAs have been suggested to prevent or compensate these impairments in transmitter side. Digital Predistortion (DPD) is a promising, useful, and cost-effective technique for achieving linearity improvement in PAs to date [1-10].

In a DPD system, the digital signal is processed by a predistorter before it is converted to analog, up-converted, and amplified [9]. The DPD technique requires both reference signal which consists of modulated symbols and feedback signal which consists of down-converted symbols from PA output. Using these signals, the DPD can be typically achieved by look-up table (LUT) algorithm. Among the DPD linearization techniques, the LUT-based DPD has been widely used because it is relatively simple and easily implemented to build the inverse function of PAs [3], [5], [10].

The receiver in the feedback path is conventionally realized using the super heterodyne technique [5], [6]. The use of this method in the predistortion loop clearly results in higher cost, larger size and more power consumption. On the other hand, the six-port receivers perform efficiently in communication systems [11-17]. The realization of the receiver using six-port technique results in a more suitable choice in the predistortion system. This is a new approach presented in [18]. This paper considers the use of a six-port receiver in the predistortion linearization loop.

With the focus on the satellite communications application in ka-band, we use the DVB-S2 [19] signal as input signal to the DPD system [7], [20]. Also, RCS+M [21], [22] supports using Continuous Carrier with DVB-S2 in the return link [23].

The remainder of the paper is structured as follows: Section Two provides an introduction to the DPD technique based on LUT. Section Three discusses six-port (five-port) receiver. We will design a typical PA and a five-port receiver for Ka-band application and evaluate the predistortion system via simulation in section Four. The results of the fabricated five-port are presented in this section. Section Five concludes the paper.

2- DIGITAL PREDISTORTION

The block diagram of a DPD system is shown in Fig. 1 (the dashed lines in Fig. 1 indicate that an address is generated based on the incoming signal). As may be seen, a DPD system is implemented in the baseband by adaptively forcing the PA to behave as a linear device.

Blocks named “gain calculation” and “coefficient error calculation and convergence control” implement the adaptation algorithm. The function of the adaptation algorithm is to derive the predistortion function, *F*. The adaptation algorithm is based upon the determination of the open loop gain, *H*, of the predistorter and amplifier combination at the power level associated with each LUT entry. The desired linear response of the predistorter and amplifier cascade requires that $F(|V_i|)G(|V_p|) = k$ (*G* is the PA function and *k* is the desired linear gain) for all inputs. Hence, if G_{lin} (which is calculated by the gain calculation block) is set to be equal to *k*, the desired open loop gain of the system is unity. If the calculated open loop gain is not equal to unity, the predistortion function must be adjusted in order to drive the open loop towards unity. This can be achieved as illustrated in the following manner in Fig. 2.

The predistortion function is defined by a set of coefficients stored in the LUT, L^n, where each n corresponds to an input signal magnitude which is mapped to an LUT address. In order to reach to the open loop gain to unity, the predistortion function coefficients are updated by dividing each coefficient by G_{lin}.

The predistortion function may be derived using either a modulated signal input (random signal) or a known training signal input. The complexity of the adaptation algorithm and its implementation can be significantly simplified, however, by using the training signal. The training signal is a tone having an increasing magnitude, i.e., ramp.

The accuracy of estimating delay in the feedback path affects the accuracy of determining the open loop gain. The input signal must be delayed precisely by an amount equal to the delay in the feedback path. The delay in the feedback path is estimated by calculating the correlation between the magnitude of the input signal and the magnitude of the feedback signal. The correlation between the input and feedback signal is performed on a modulated signal because the gain compression of the amplifier makes the accuracy of the correlation over the training signal suspect. In addition, because the envelope of the modulated signal will typically have a PDF such that it spends much of its time within the linear operating region of the amplifier, correlation using the modulated signal becomes more reliable. However, because the modulated signal is stochastic, the statistics of the modulated signal, as well as the size of the data block over which the correlation operation is performed will impact the accuracy of the delay estimation. In general, the accuracy of the estimation improves as the block sizes increases. Unfortunately, a larger block size requires more memory and takes longer to perform the estimate.

The process of down-conversion and demodulation in the feedback path is realized by using a six-port structure.

3- SIX-PORT STRUCTURE

As shown in Fig. 1 a receiver is required in the feedback path in a predistortion linearization system. To this purpose, the six-port (five-port) receiver is introduced in this section. Using this kind of receiver in the feedback path of the predistorter structure results in lower costs and

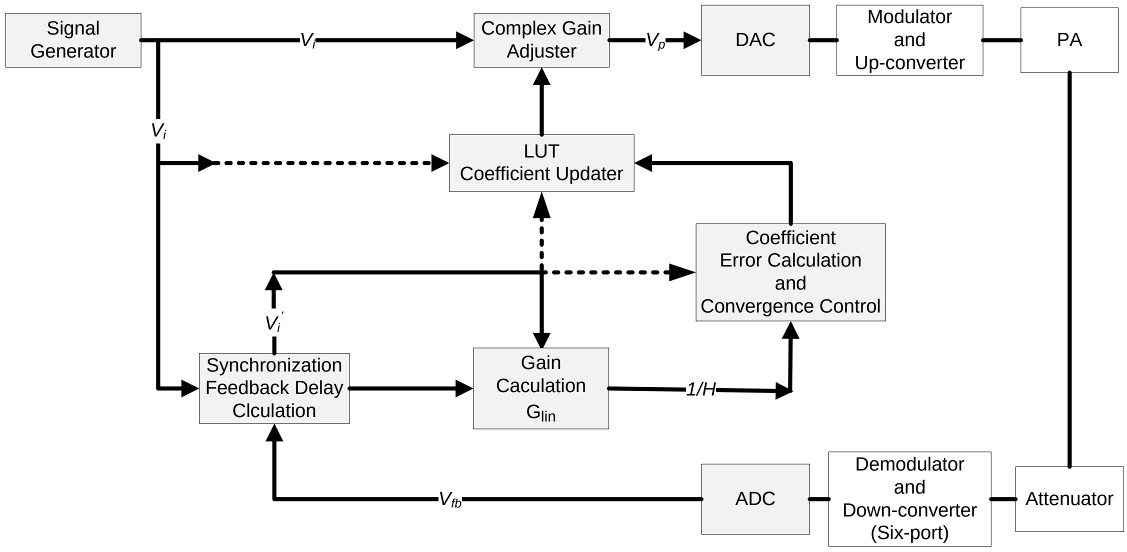

Fig. 1. Look-up table adaptive digital predistorter, $\frac{1}{H}=\frac{V_i'}{V_{fb}}=\frac{G_{lin}}{F(|V_i|)G(|V_p|)}$

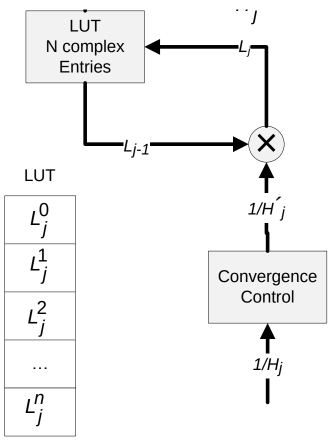

Fig. 2. Calculation of new predistortion function.

less complexity [11].

A six-port receiver consists of two inputs and 4 outputs. In direct-conversion receiver applications, the *RF* and *LO* signals are applied to two input ports as two complex signals. The passive six-port structure produces 4 combinations of *RF* and *LO* signals and injects them to 4 power detectors. *I* and *Q* components (of the *RF* signal) can be extracted after some simple operations on the 4 resulted output powers [16]. For symmetrical structures, the relation between *I* and *Q* and output powers can be written as follows:

$$I = C(P_5 - P_3) \tag{1}$$

$$Q = C(P_4 - P_6) \tag{2}$$

$$I + Q = 2C(P_4 - P_3) = 2C(P_5 - P_6) \tag{3}$$

where *C* is a frequency dependent parameter.

A five-port receiver results from removing one port from a six-port receiver. In the five-port structure, the calculated *I* is used in determining *Q* or vice versa. For example, if we calculate P_6 from (3) and substitute it into (2), *Q* would be determined. It means port 6 has been removed. Demodulation equations in this case are

$$I = C(P_5 - P_3) \tag{4}$$

$$Q = 2C(P_4 - [P_5 - I/2C]) \tag{5}$$

This method has the advantage of reducing the number of power detectors and ADCs, thereby reducing costs. The functional block diagram of a five-port structure is shown in Fig. 3.

4- SIMULATION AND RESULTS

To evaluate the performance of the DPD system, we have designed a typical PA in the ka-band. After some specific amount of attenuation, the output of PA is down-converted and demodulated by a five-port receiver. The predistortion function is produced with DSP blocks.

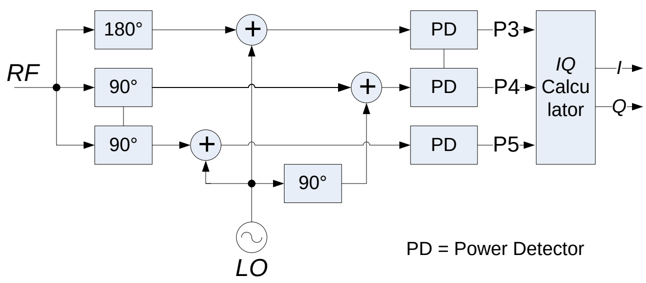

Fig. 3. Functional block diagram of five-port structure.

A- POWER AMPLIFIER LAYOUT IN KA-BAND

millimeter wave HEMT to design the PA [24], [25]. The PA operates at deep Class AB. We planned the input and output distributed microstrip matching networks on 10 mil RO3003 substrate with ε_r=3. The resulting schematic of the PA is shown in Fig. 4. The power performance of the PA was determined by harmonic balance nonlinear analysis (as depicted in Fig. 5).

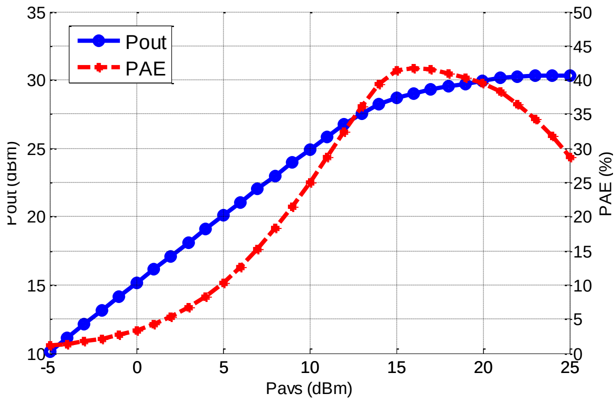

Fig. 5. Power performance of Ka-band power amplifier in f = 27.5 GHz.

The PA exhibits power of 30.03 dBm and 39.58 %

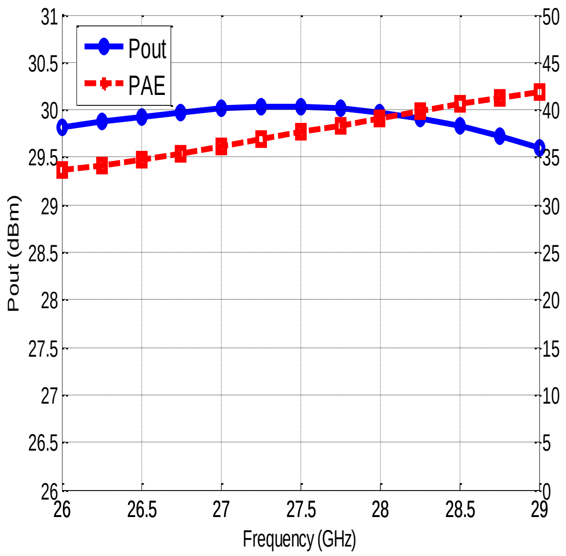

Fig. 6. Output power and efficiency vs frequency in Pavs = 20 dBm.

PAE at 27.5 GHz and 20 dBm Pavs. Output power and efficiency as functions of frequency at a given input power can be seen in Fig. 6. These simulation results

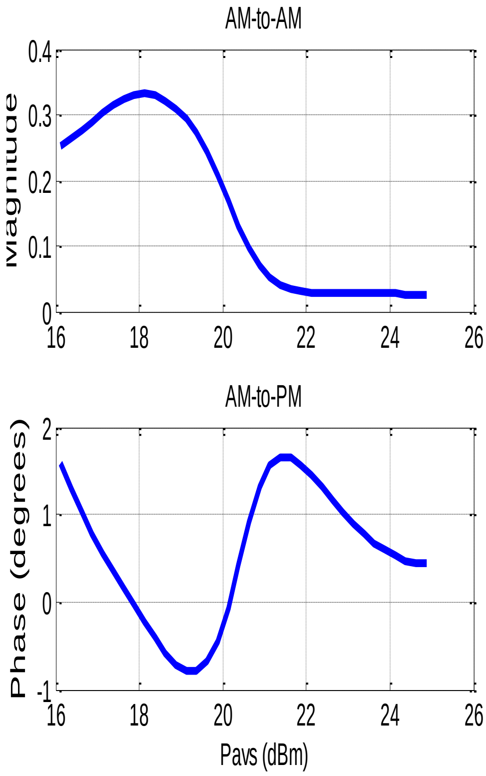

Fig. 7. AM-AM and AM-PM characteristics in f = 27.5 GHz.

suggest that the designed Ka-band PA is suitable for ground terminal in order to close a return link As the predistortion correction is done on amplitude and phase, we have plotted AM-to-AM and AM-to-PM characteristics of the PA in Fig. 7

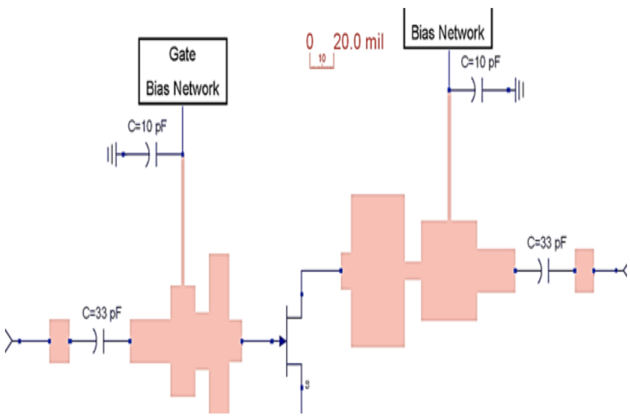

Fig. 4. Ka-band power amplifier

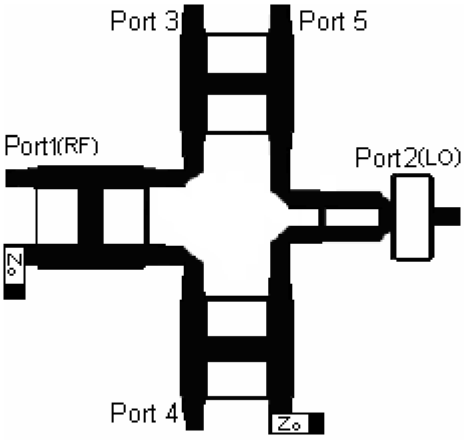

Fig. 8. Five-port architecture layout.

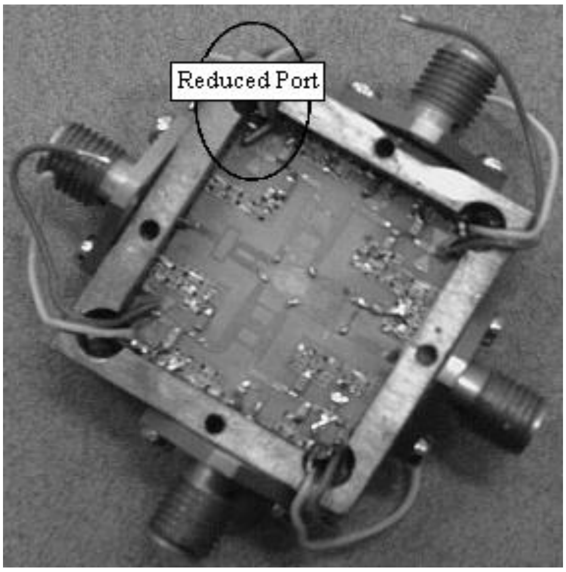

Fig. 9. Photograph of Five-port receiver.

B- FIVE-PORT IN KA-BAND

A five-port receiver was designed and fabricated to be used in the feedback path of the predistortion system. This receiver operates in 23-29 GHz. Its microstrip circuit consists of extreme broadband components: a Wilkinson power divider and three quadrature hybrids (Fig. 8).

Fig. 9 shows the photograph of the fabricated five-port structure [16]. This circuit was fabricated on 10 mil RO3003 substrate with ε_r=3 (the same substrate as used for the matching networks). The accuracy of the transmission lines is ±50 μm. This uncertainly results in some changes in the S-parameters. Therefore, there would be imbalance in transmission magnitude and phase. The intrinsic need for calibration of multi-port receivers removes these imbalances. Fig. 10a shows the measured S-parameters of the fabricated five-port. Due to microstrip loss, transmission is found to be about -10 dB. Isolation better than 20 dB in the whole frequency band and -40 dB in the center frequency accomplished. Fig. 10b shows the absolute measured phase shift from the input ports to port 3 and port 4. The aimed $90°$ phase difference between RF signals at port 3 and port 4 achieved and LO signal had same phase shift at output ports.

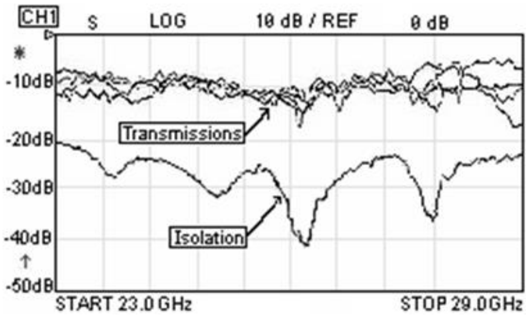

(a)

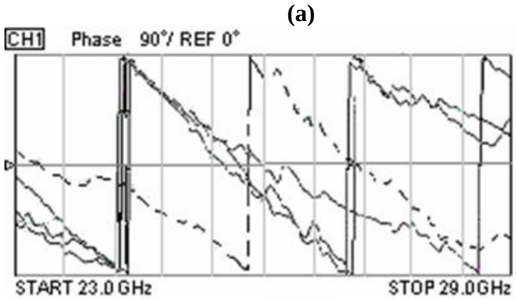

(b)

Fig. 10. (a) Measured S-parameters of the Five-port , (b) Absolute measured phase shift from the input ports to the ports 3 and 4

C- DIGITAL PREDISTORTION SIMULATION

The block diagram of Fig. 1 shows the simulation platform of the DPD system. The platform implemented using ADS software and analyzed with co-simulation of Data Flow controller and circuit-envelope simulator.

Although significant improvement in the ACPR of the amplifier should be observed even after a single training ramp, yet simulations have shown that the predistortion function can converge to a solution after only six training ramps. The LUT is implemented using the LUT_RAM and the number of entries in the LUT is taken as 256. The final magnitude and phase LUT entries have been shown in Fig. 11. The magnitude and phase plotted in this figure are associated with the inverse of AM-AM and AM-PM characteristics of the PA.

Fig. 12 shows the delay calculation between input signal and feedback signal. The rising portion of the ramp is used by the adaptation algorithm in the calculation of the predistortion function. With the precise delay of the input signal, the input signal and the feedback signal have been synchronized.

Input signal (DVBS2 with QPSK ¾ modulation and coding rate, respectively) and the PA output signal are plotted in Fig. 13. The output signal is similar to the linear amplified version of the input signal with little distortion. The spectrum of the output with and without predistortion is shown in Fid. 14. The third order intermodulation products reduce about 43 dB and the fifth order intermodulation products reduce about 25 dB after DPD of the PA. The resulting spectrum of the output signal shows significant reduction of the intra-system interference to the adjacent networks which is mainly due to the nonlinearity effects of the PA.

5- CONCLUSION

The use of a five-port receiver in a new DPD linearization system for PAs was described. A digital LUT-based adaptive predistortion system was used to linearize nonlinear characteristics of a PA designed in Ka-band. Using the five-port receiver in place of the classic heterodyne receiver reduces cost and complexity of implementation. The new proposed digital adaptive predistortion configuration is easy to implement. The results show a significant reduction in ACPR and an improvement in linearity.

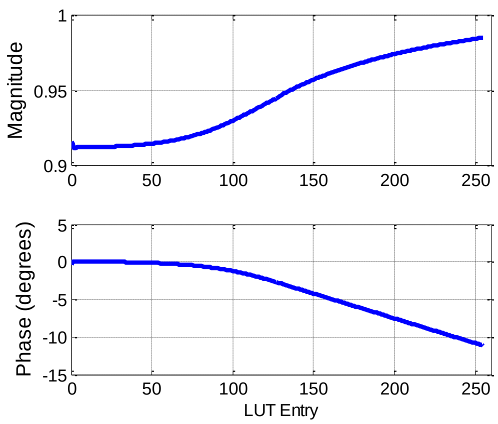

Fig. 11. Final magnitude and phase entries of LUT (iteration 6).

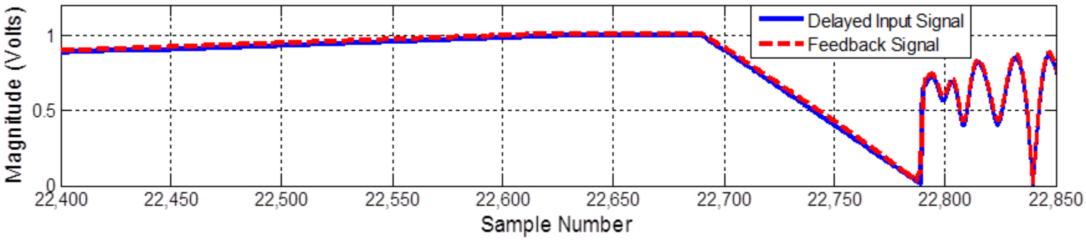

Fig. 12. Delay between input signal and feedback signal.

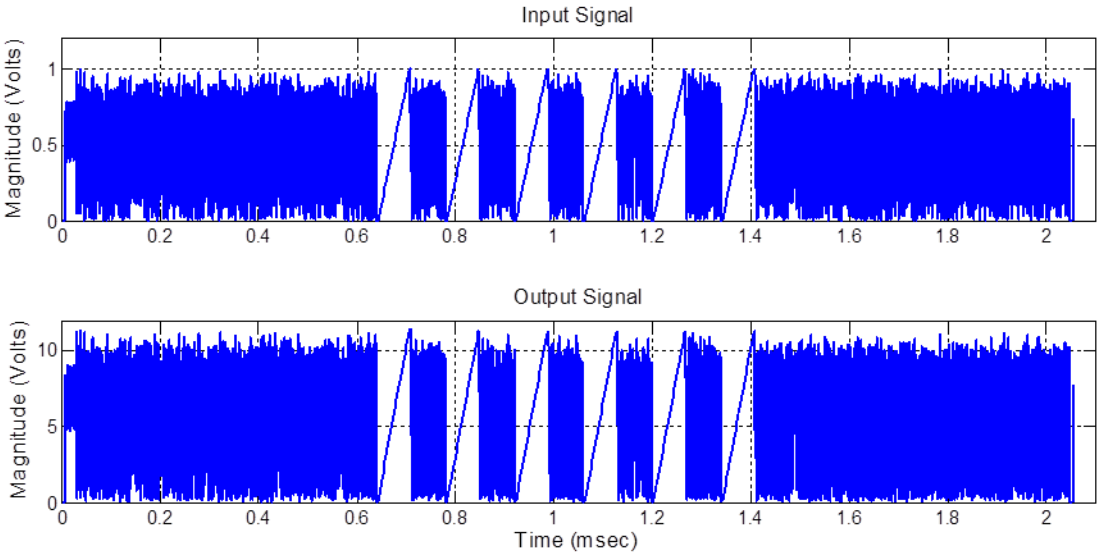

Fig. 13. Time domain signals.

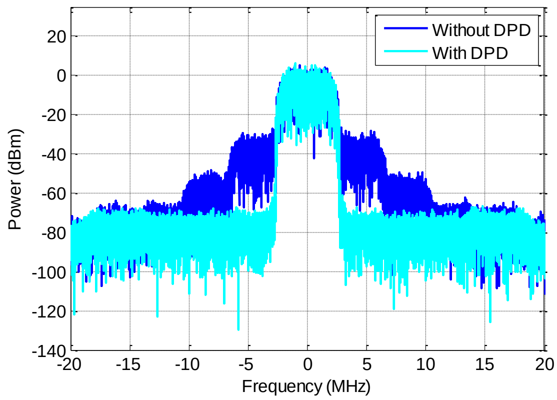

Fig. 14. Spectrum of output signal with and without predistortion

6- REFERENCES

[1] Cripps, S.C, “Power Amplifier Linearization Techniques”, in Power Amplifiers for Wireless Communications, 2nd Edition. Boston, MA: Artech, 2006.

[2] Cripps, S.C, “Predistortion Techniques” in Advanced Techniques in RF power amplifier Design Boston, MA: Artech, 2002.

[3] G. Montoro, P. L. Gilabert, E. Bertran, A. Cesari, and D. D. Silveira, “A New Digital Predictive Predistorter for Behavioral Power Amplifier Linearization”, IEEE Microw. Wireless Compon. Lett., vol. 17, no. 2, pp. 448– 450, 2007.

[4] Y. Liu, J. Zhou, W. Chen, and B. Zhou, “A Robust Augmented Complexity-Reduced Generalized Memory Polynomial for Wideband RF Power Amplifiers”, IEEE Trans. Ind. Electron., vol. 61, no 5. 2389- 2401, pp. 2389- 2401, 2013.

[5] L. Jaekwon, J. Sungho, K. Junghyun, and S. Toung-Woo, “Adaptive HPA Linearization Technique for Practical ATSC DTV System”, IEEE Trans. Broadcast., vol. 59, no. 2, pp. 376-381, 2013.

[6] F. F. Tafuri, C. Guaragnella, M. Fiore, and T. Larsen, “Linearization of RF Power Amplifiers Using an Enhanced Memory Polynomial Predistorter”, NORCHIP, pp. 1- 4, 2012.

[7] A. S. Kondrashov, “Digital Predistortion in On-Board Satellite System Power Amplifiers”, Mediterranean Conference on Embedded Computing (MECO), pp. 200- 203, 2012.

[8] X. Dian and Z. Zhibin, “An Improved Adaptive Algorithm for Digital Predistortion”, International Conference on Computer Science and Electrical Engineering, pp. 340- 343, 2012.

[9] J. Hong, Y. Xin, and P. A. Wilfor, “Digital Predistortion Using Stochastic Conjugate Gradient Method”, IEEE Trans. Broadcast., vol. 58, no. 1, pp. 114- 124, 2012.

[10] Y. Y. Woo, J. Kim, J. Yi, S. Hong, I. Kim, J. Moon, and B. Kim, “Adaptive Digital Feedback Predistortion Technique for Linearizing Power Amplifiers”, IEEE Trans. Microw. Theory Tech., vol. 55, no. 5, pp. 932- 940, 2007.

[11] F. M. Ghannouchi and A. Mohammadi, Six-Port Technique with Microwave and Wireless Applications. Norwood, MA: Artech, 2009.

[12] R. Mirzavand, A. Mohammadi, and F. M. Ghannouchi, “Five-Port Microwave Receiver Architectures and Applications”, IEEE Commun. Mag., vol. 48, no. 6, pp. 30- 36, 2010.

[13] M. Mohajer, A. Mohammadi, and A. Abdipour, “Direct Conversion Receivers Using Multi-Port Structures for Software Defined Radio Systems”, IET Microw. Antenna P., vol. 1, no. 2, pp. 363–372, 2007.

[14] B. Luo and M. Y. W. Chia, “Performance Analysis of Serial and Parallel Six-Port Modulators”, IEEE Trans. Microw. Theory Techn., vol. 56, no. 9, pp. 2062- 2068, 2008.

[15] R. G. Bosisio et al., “New-Wave Radio”, IEEE Microw. Mag., vol. 9, no. 1, pp. 89– 100, 2008.

[16] R. Mirzavand, A. Mohammadi, and A. Abdipour, “Five-Port Software-Defined Radio Receiver Implementation in Ka-Band”, Microwave Conference, APMC, pp. 480- 483, 2006.

[17] N. V. Sani, A. Mohammadi, A. Abdipour, and F. M. Ghannouchi, “Analysis of Multiport Receivers Using FDTD Technique”, J Electromagnet. Wave, vol. 23, no. 5- 6, pp. 635- 643, 2009.

[18] M.R. Beikmirza, A. Mohammadi, R. Mirzavand, “An adaptive pre-distortion linearization technique for power amplifier using a five-port receiver”, Telecommunications (IST), 2014 7th International Symposium on, pp.1040- 1045, 2014.

[19] ETSI EN 302 307 V1.1.2, “Digital Video Broadcasting (DVB)”, European Standard (Telecommunications series), 2006.

[20] M. Cote, L. Erup, M. Lambert, and N. McSparron, “Implementation Challenges and Synergistic Benefits of DVB-S2 & DVB-RCS”, The Institution of Engineering and Technology Seminar on Digital Video Broadcasting over Satellite: Present and Future, pp. 21- 34, 2006.

[21] H. Skinnemoen and P. Thompson, “Overview of DVB- RCS+M and its Development”, Int. J. Satell. Co. Netw., vol. 28, no. 3- 4, pp. 119-135, 2010.

[22] H. Skinnemoen, “Introduction Special Issue on DVB-RCS+M”, Int. J. Satell. Co. Netw., vol. 28, no. 3- 4, pp. 119- 135, 2010.

[23] H. Skinnemoen, “Creating the Next Generation DVB-RCS Satellite Communication & Applications”, ASMA/SPSC, pp. 147- 154, 2010.

[24] I. Angelov, H. Zirath, and N. Rorsmann, “A New Empirical Nonlinear Model for HEMT and MESFET Devices”, IEEE MTT, vol. 40, no. 12, pp. 2258- 2266, 1992.

[25] I. Angelov, L. Bengtsson, and M. Garcia, “Extensions of the Chalmers Nonlinear HEMT and MESFET Model”, IEEE MTT, vol. 44, no. 10, pp. 1664- 1674, 1996.